Peptides 71 (2015) 276–285

Contents lists available at ScienceDirect

Peptides

journal homepage: www.elsevier.com/locate/peptides

# High throughput screening methods for assessing antibiofilm and immunomodulatory activities of synthetic peptides

Evan F. Haney, Sarah C. Mansour, Ashley L. Hilchie, César de la Fuente-Núñez, Robert E.W. Hancock*

*Center for Microbial Diseases and Immunity Research, Department of Microbiology and Immunology, University of British Columbia, Vancouver, British Columbia, Canada*

ARTICLE INFO

*Article history:*
Received 27 January 2015
Received in revised form 17 March 2015
Accepted 19 March 2015
Available online 31 March 2015

*Keywords:*
Antibiofilm peptide
Immunomodulatory peptide
Bacterial biofilms
Peptide optimization

ABSTRACT

The recent observation that certain cationic peptides possess potent antibiofilm activity demonstrated that small peptides could be used to treat biofilm-associated infections. Other so-called innate defense regulator peptides possess potent immunomodulatory properties such as leukocyte recruitment and suppression of harmful inflammation. A peptide that directly targets biofilm cells while favorably modulating the immune response would be particularly advantageous for treating serious skin infections caused by *Staphylococcus aureus*. In the present work, using SPOT-synthesized peptide arrays on cellulose membranes, we outline a strategy for systematically assessing the antibiofilm activity of hundreds of IDR-1002 (VQRWLIVWRIRK-$NH_2$) and IDR-HH2 (VQLRIRVAVIRA-$NH_2$) peptide variants against MRSA biofilms. In addition, the ability of these peptides to stimulate production of a monocyte chemoattractant protein (MCP-1) and suppress LPS-induced interleukin (IL)-1β production in human peripheral blood mononuclear cells (PBMCs) was evaluated. These results informed the synthesis of second-generation peptides resulting in a new peptide, IDR-2009 (KWRLLIRWRIQK-$NH_2$), with enhanced MCP-1 stimulatory activity, favorable IL-1β suppression characteristics and strong antibiofilm activity against MRSA and *Pseudomonas aeruginosa* biofilms. This work provides a proof-of-concept that multiple peptide activities can be optimized simultaneously to generate novel sequences that possess a variety of biological properties.



## Introduction

*Staphylococcus aureus* is a Gram positive bacterium that is frequently isolated from the skin and respiratory tract. While colonization is observed in 20% of the population, a small proportion can develop symptomatic skin infections [1]. These infections typically present as small red bumps, a rash or painful pus-filled boils or abscesses. While most of these infections are localized to the skin and soft tissues, others can spread rapidly throughout the body, causing a variety of life-threatening diseases such as sepsis, toxic shock syndrome and necrotizing pneumonia [2]. The emergence of methicillin resistant *S. aureus* (MRSA) strains in hospital settings and within the community [3] has made treating *S. aureus* infections exceedingly difficult in recent years, leading to significant increases in costs related to hospitalization and treatment [4]. The current treatment regimen for MRSA infections in hospitalized patients consists of intravenous administration of vancomycin. Unfortunately, vancomycin resistance has already emerged [5,6], which highlights the continuing need to develop novel antimicrobial compounds to combat MRSA-associated infections.

Antimicrobial peptides (AMPs) have long been studied as a potential reservoir for novel antimicrobial compounds. AMPs are evolutionarily conserved molecules of the innate immune system that are found in all life forms [7,8]. AMPs are short peptide sequences, typically 12–50 residues in length [9], characterized by a high proportion of hydrophobic and positively charged residues that gives them an overall cationic charge [10]. Naturally occurring AMPs have been found to play a role in preventing *S. aureus* infections in vivo. For instance, keratinocyte derived RNAse 7 plays an important role in cutaneous defense and prevents *S. aureus* infection within the skin [1]. In addition, pathogenic *S. aureus* has been

*Abbreviations:* AMP, antimicrobial peptide; BM2, basal medium 2; CD, circular dichroism; DPC, dodecylphosphocholine; ELISA, enzyme linked immunosorbent assay; HDP, host defense peptide; IDR, innate defense regulator; IL-1β, interleukin-1 beta; LDH, lactate dehydrogenase; LPS, lipopolysaccharide; MCP-1, monocyte chemotactic protein 1; MRSA, methicillin resistant *Staphylococcus aureus*; PBMC, peripheral blood mononuclear cell; SDS, sodium dodecyl sulphate.

* Corresponding author at: Centre for Microbial Diseases and Immunity Research, 2259 Lower Mall Research Station, UBC, Vancouver, BC, Canada V6T 1Z4. Tel.: +1 604 822 2682.
*E-mail address:* bob@hancocklab.com (R.E.W. Hancock).

http://dx.doi.org/10.1016/j.peptides.2015.03.015
0196-9781/

shown to induce production of human beta defensin (hBD)-1 and hBD-3 from keratinocytes [11] and hBD-3 possesses bactericidal activity toward MRSA [12]. Along these lines, patients with atopic dermatitis, an inflammatory skin disease, are more likely to be colonized and infected with *S. aureus*, and this has been partly attributed to reduced expression of hBDs as well as the cathelicidin, LL-37 [13]. Moreover, low RNAse 7 expression in healthy humans has been associated with *S. aureus* colonization [1] and people deficient in hBD-3 expression are more susceptible to persistent nasal colonization with *S. aureus* [14].

Several synthetic peptides have been evaluated for their direct antibacterial activity against planktonic MRSA. Most of this work has focused on identifying natural peptides and optimizing synthetic variants for their direct antimicrobial activity or generating novel sequences based on common physico-chemical properties of AMPs [15]. Recent examples include LL-37 peptide variants that could be used to treat Staphylococcal infections in burn wounds [16] or a truncated peptide variant of a natural sea urchin peptide, centrocin 1, that exhibits in vivo activity against *S. aureus* and MRSA [17]. While some peptides show promise as novel antibiotics, generally speaking, they have been optimized for their ability to kill planktonic (free swimming) bacteria. However, bacterial infections, particularly those associated with skin infections, are often the result of bacterial communities known as biofilms.

Biofilms are a persistent multicellular community of bacteria encased in an extracellular matrix that can adhere to and grow on almost any surface [18]. Biofilms confer increased resistance to many antimicrobials [18], making them exceedingly difficult to treat with conventional antibiotics. There is increasing evidence that biofilms are often associated with dermal wounds [19], and that their presence prolongs infection and prevents normal wound healing [20]. Indeed, it is estimated that biofilms are responsible for up to 65% of all infections in humans [21,22]. Therefore, specifically targeting bacterial cells within a biofilm may be an effective strategy to combat serious biofilm-associated infections. Interestingly, certain antimicrobial peptides have been recently found to possess activity against biofilms that is independent of their activity against planktonic bacteria. For instance, human LL-37, a poorly active antimicrobial, prevents biofilm formation in *Pseudomonas aeruginosa* [23]. Additionally, smaller synthetic peptides have also been identified with potent antibiofilm activity such as 1037, which blocks biofilm formation at sub-MIC concentrations of peptide [24] as well as 1018 (also termed IDR-1018 for its immunomodulatory properties – see below), which exhibits potent antibiofilm activity against a range of bacterial species, including *S. aureus* [25]. Critically, both of these peptides are active against *Burkholderia* biofilms that are completely resistant to peptides when growing planktonically.

Many cationic peptides lose their antimicrobial activity under physiological conditions due to antagonism by divalent cations and polyanions, organs and other body fluids [26], which limits their clinical potential. In contrast, under these same conditions, such peptides often exhibit potent and multifaceted immunomodulatory functions and it is becoming increasingly appreciated that this type of activity might be the primary mechanism by which these peptides protect against infection and inflammation in vivo [7,27]. For this reason, the term host defense peptide (HDP) is often used as a group term to describe peptides accommodating their various functions in host defences (cf. the term AMP that implies just direct planktonic antimicrobial activity). Synthetic analogs are termed innate defense regulator (IDR) peptides.

Several synthetic IDRs with strong immunomodulatory activities have been identified by our group and others. Most notably, in addition to the potent antibiofilm activity described above, IDR-1018 possesses strong immunomodulatory properties [28] and promotes wound healing [29]. While immunomodulatory peptides share many characteristics with conventional AMPs, very little is known about the specific sequence requirements that mediate the immunomodulatory abilities of HDPs. In fact, as also found for other peptides [23,24], the peptide characteristics that govern antibiofilm and immunomodulatory activity are fundamentally different from the antimicrobial characteristics since IDR-1018 exhibits relatively weak antibacterial activity versus planktonic cells [25]. Curiously, in our experience, there appears to be significant sequence overlap between antibiofilm and immunomodulatory peptides, suggesting a similar sequence requirement for both, possibly since they must both be internalized into cells. Therefore, the objective of the current work was to develop a method to simultaneously optimize the antibiofilm and immunomodulatory activities of cationic peptides.

The classical approach to optimize AMPs for their antibacterial activity involves synthesizing small peptide libraries that substitute certain amino acids in the parent peptide to improve physico-chemical characteristics that contribute to improved antibacterial activity. This rational design strategy depends on extensive empirical information collected over many years. In contrast, the immunomodulatory and antibiofilm activities of HDPs have only recently become appreciated and only a modest number of peptide sequences have been studied for their immunomodulatory and/or antibiofilm properties. Consequently, very little is known about the overall sequence requirements that define these biological activities. Therefore, the typical optimization strategy used to rationally design AMPs by mutating individual residues to improve specific chemical properties cannot be employed. In addition, synthesizing large numbers of peptides at sufficient quantities to adequately understand these sequence requirements is prohibitively expensive. As a result, no large-scale studies addressing this question have been published to date. Therefore, using as starting sequences two synthetic IDRs previously identified by our group, namely IDR-1002 and IDR-HH2, we have utilized SPOT-synthesized peptide arrays to systematically assess and concurrently improve the immunomodulatory and antibiofilm activities of these synthetic peptides. Both IDR-1002 (VQRWLIVWRIRK-$NH_2$) and IDR-HH2 (VQLRIRVAVIRA-$NH_2$) have immunomodulatory properties [30–35] while their antibiofilm activity against *S. aureus* has yet to be elucidated.

Using SPOT-synthesized peptides on cellulose membranes, single amino acid substitution libraries of IDR-1002 and IDR-HH2 were generated substituting the nine constituent amino acids of both peptides (R, K, Q, G, A, W, V, L, I) at every position along the length of each peptide. All these derivatives were then assayed for their antibiofilm activity against a clinical isolate of MRSA using a static microtitre 96-well plate assay. At the same time, the ability of each peptide to stimulate monocyte chemotactic protein 1 (MCP-1) production and suppress lipopolysaccharide (LPS)-induced interleukin (IL)-1β production from human peripheral blood mononuclear cells (PBMCs) was assessed. All of this data was used to generate substitution matrices for both IDR-1002 and IDR-HH2 which informed the synthesis of next generation peptides. Mutations that were found to improve MCP-1 production and suppress LPS-induced IL-1β production from PBMCs as well as increasing MRSA antibiofilm activity were combined and incorporated into the new peptides. The biological activity profiles of the next generation peptides were evaluated, one of which demonstrated an improved therapeutic potential.

## Materials and methods

### *Peptide synthesis and peptide stock solution preparation*

SPOT-synthesis of peptide arrays on cellulose membranes was performed by Kinexus Inc. (Vancouver, BC, Canada) as described

previously [36–38]. Each peptide spot was assumed to have a density of 100 nmol and a peptide purity of 60–70%, based on previous measurements of the amounts of peptides created per spot. Peptides were solubilized in 200 μl of sterile water (Baxter International. Deerfield, IL) and incubated at 23 °C for ~2 h with gentle shaking. The resulting (~200 μM) stock peptide solutions were used directly or serially diluted into endotoxin free water for the antibiofilm and immunomodulatory screens, described below. Synthetic peptides of the second generation peptides as well as IDR-1002 and IDR-HH2, were obtained at 95% purity from Genscript (Piscataway, NJ). Stock solutions of these peptides were prepared to 1 mg/ml in sterile water.

*Antibiofilm activity screen*

The antibiofilm activity of the IDR-1002 and IDR-HH2 single amino acid variants was assessed using a static microtitre plate assay, as described previously [23,24,39]. Briefly, an overnight culture of MRSA SAP0017 (Clinical isolate kindly provided by Dr. Tony Chow at Vancouver General Hospital) was diluted 1/100 in tryptic soy broth supplemented with 1% glucose and 97.5 μl was added to each well of a 96-well Costar polypropylene plate (Corning Inc., Corning, NY) containing 2.5 μl of peptide diluted in water or water alone. Each peptide was evaluated for antibiofilm activity at concentrations of ~5, 2.5, 1.25 and 0.6125 μM. After overnight growth, the planktonic cells were washed away with deionized water and the remaining adhered biomass was stained with 0.1% crystal violet, washed with water and solubilized in 70% ethanol. Total biofilm mass was quantified by measuring the optical density (OD) at 595 nm using a microtiter plate reader (Bio-Tek Instruments Inc., Winooski, VT). The percent biofilm inhibition was calculated in relation to the amount of MRSA biofilm grown in the absence of peptide (defined as 100%) and the media sterility control (defined as 0% growth). Results from three separate biological replicates were averaged and outliers were identified and removed from the analysis using a modified Thompson Tau test.

*Biofilm growth in flow cells*

Using a peristaltic pump, 3-channel flow cell chambers (IBI Scientific. Peosta, IA) were initially filled with minimal BM2 glucose medium [62 mM potassium phosphate buffer, pH 7, 7 mM $(NH_4)_2SO_4$, 2 mM $MgSO_4$, 10 μM $FeSO_4$ and 0.4% (wt/vol) glucose] and subsequently injected with 1/20 dilutions of overnight bacterial cultures. The cells were allowed to adhere to the plastic surface of the flow cell chamber for 2 h under static conditions. The biofilms were then matured by pumping BM2 media through the system at a constant flow rate of 2.4 ml/h for 72 h. Peptide was added to the system two days after the initial bacterial injection and then pumped through the flow cells for the final 24 h. Three days after inoculation, the flow cell channels were injected with fluorescent stains SYTO-9 and propidium iodide to image total and dead cells respectively using an Olympus FluoView FV1000 confocal laser scanning microscope (Olympus Corp., Tokyo, Japan). Three-dimensional images were constructed and analyzed using Imaris software (Bitplane AG, Belfast, UK).

*Purification and treatment of PBMCs*

PBMCs were isolated from healthy human donors as described previously [40]. Cells were seeded to a final density of $1 \times 10^6$ cells/ml in 96-well flat bottom tissue culture treated plates (Corning Incorporated, Corning, NY) and were stimulated with vehicle control or with 10 ng/ml *P. aeruginosa* PAO1 LPS. SPOT-synthesized peptides and the second-generation peptides were added to the PBMCs at concentrations of ~2, 10 and 20 μM or 5, 25 and 50 μg/ml respectively. In all experiments, the total volume per well was 100 μl. Treated PBMCs were incubated overnight at 37 °C in a 5% $CO_2$ humidified atmosphere and the supernatants were collected in fresh 96-well plates following centrifugation at 1150 rpm for 5 min. Sample supernatants were either used immediately in the lactate dehydrogenase (LDH) assay or frozen at −20 °C for cytokine quantification by enzyme linked immunosorbent assays (ELISA).

*LDH release assay*

Peptide toxicity to PBMCs was assessed using the LDH-release assay (Roche Diagnostics, Basel, Switzerland) following manufacturers' instructions. Vehicle treated samples and 2% (v/v) Triton X-100 treated samples served as the negative and positive controls, respectively. Cytotoxicity results represent the mean LDH release ($n = 5$).

*ELISA*

ELISAs were used to quantify the levels of MCP-1 and IL-1β production by PBMCs. All sandwich ELISA kits were purchased from eBioscience, Inc. (San Diego, CA). ELISAs were carried out on three separate biological replicates in the immunomodulatory screen and at least 4 separate biological repeats when evaluating the activity of the second generation peptides.

*Circular dichroism spectroscopy*

Circular dichroism spectra were acquired on a Jasco J810 Spectropolarimeter (Jasco Inc., Easton, MD). All spectra were acquired in 25 mM sodium phosphate buffer (pH 7.4) using a peptide concentration of 25 μM. In addition, peptide samples were prepared in the presence of 10 mM DPC or 25 mM SDS detergent micelles. Far-UV CD spectra were acquired between 260 and 190 nm using a 0.5 nm step size and a scanning speed of 100 nm/min. The bandwidth was set to 1 nm and the response was set to 2 s. Final spectra are the accumulated average of three separate scans. The raw CD data was converted to mean residue ellipticities as described by Wallace and Janes [41].

## Results

*Antibiofilm and immunomodulatory activity of IDR-1002 and IDR-HH2 derivatives*

The results from the antibiofilm and immunomodulatory screens revealed that there was a wide distribution of activities among IDR-1002 and IDR-HH2 derivatives (Supplementary Figures 1 and 2). The antibiofilm activities were assessed at four different peptide concentrations, and ranking the peptides from most active to least active revealed that the IDR-1002 and IDR-HH2 derivatives had roughly similar activity distributions (Supplementary Figure 1). The percent biofilm inhibition observed at a peptide concentration of ~2.5 μM yielded the largest separation between the most and least active peptides, therefore the data from this concentration was used to generate antibiofilm substitution matrices for IDR-1002 and IDR-HH2 (Fig. 1A).

Looking at each peptide individually, it appeared that decreasing the number of hydrophobic amino acids between residues 4 and 10 of IDR-1002 negatively impacted on the antibiofilm activity of the peptide. This was particularly true for substitutions at W4, I6, W8 and I10 since cationic, polar or small amino acids were poorly tolerated at each of these positions. The exception to this was residue L5, which appeared to tolerate most amino acid substitutions while still exerting comparatively strong biofilm inhibition. Additionally,

A

| Anti-biofilm | Sub. Amino Acid | 1002 Sequence | | | | | | | | | | | |
|---|---|---|---|---|---|---|---|---|---|---|---|---|---|
| | | V | Q | R | W | L | I | V | W | R | I | R | K |
| Cationic | R | 33 | 40 | 27 | 64 | 38 | 87 | 42 | 77 | 27 | 85 | 27 | 38 |
| | K | 25 | 31 | 39 | 113 | 21 | 98 | 72 | 131 | 50 | 129 | 26 | 27 |
| Polar | Q | 23 | 27 | 30 | 64 | 52 | 78 | 55 | 80 | 59 | 61 | 33 | 35 |
| Small, Hydro-phobic | G | 32 | 26 | 44 | 58 | 41 | 74 | 46 | 58 | 56 | 65 | 40 | 50 |
| | A | 45 | 32 | 35 | 48 | 30 | 72 | 42 | 48 | 42 | 55 | 48 | 63 |
| Large, Hydro-phobic | W | 24 | 39 | 32 | 27 | 24 | 47 | 38 | 27 | 27 | 29 | 63 | 29 |
| | V | 27 | 28 | 51 | 31 | 25 | 29 | 27 | 44 | 53 | 37 | 32 | 33 |
| | L | 31 | 28 | 41 | 67 | 27 | 48 | 43 | 43 | 43 | 35 | 39 | 36 |
| | I | 36 | 30 | 38 | 38 | 16 | 27 | 27 | 31 | 47 | 27 | 33 | 34 |

| Anti-biofilm | Sub. Amino Acid | HH2 Sequence | | | | | | | | | | | |
|---|---|---|---|---|---|---|---|---|---|---|---|---|---|
| | | V | Q | L | R | I | R | V | A | V | I | R | A |
| Cationic | R | 47 | 46 | 107 | 30 | 108 | 30 | 97 | 29 | 35 | 27 | 30 | 20 |
| | K | 45 | 31 | 86 | 35 | 73 | 36 | 93 | 27 | 48 | 32 | 57 | 33 |
| Polar | Q | 43 | 30 | 72 | 55 | 75 | 65 | 79 | 35 | 57 | 39 | 37 | 28 |
| Small, Hydro-phobic | G | 35 | 34 | 79 | 60 | 66 | 67 | 67 | 46 | 41 | 42 | 28 | 31 |
| | A | 44 | 31 | 48 | 58 | 55 | 59 | 43 | 30 | 49 | 47 | 36 | 30 |
| Large, Hydro-phobic | W | 33 | 30 | 38 | 42 | 37 | 44 | 30 | 25 | 25 | 52 | 55 | 42 |
| | V | 30 | 23 | 43 | 40 | 50 | 61 | 30 | 34 | 30 | 32 | 49 | 35 |
| | L | 28 | 31 | 30 | 46 | 42 | 82 | 32 | 50 | 35 | 37 | 53 | 49 |
| | I | 27 | 46 | 38 | 53 | 30 | 55 | 31 | 26 | 27 | 30 | 45 | 35 |

B

| IL-1β | Sub. Amino Acid | 1002 Sequence | | | | | | | | | | | |
|---|---|---|---|---|---|---|---|---|---|---|---|---|---|
| | | V | Q | R | W | L | I | V | W | R | I | R | K |
| Cationic | R | 0.47 | 0.71 | 0.68 | 1.12 | 1.18 | 1.20 | 1.21 | 1.01 | 0.68 | 0.87 | 0.68 | 0.86 |
| | K | 0.40 | 0.67 | 0.67 | 1.18 | 1.46 | 1.13 | 1.25 | 1.04 | 0.92 | 0.93 | 0.79 | 0.68 |
| Polar | Q | 0.65 | 0.68 | 0.44 | 1.16 | 1.25 | 1.25 | 1.24 | 1.25 | 1.14 | 0.98 | 0.90 | 0.95 |
| Small, Hydro-phobic | G | 0.65 | 0.72 | 0.63 | 0.90 | 1.23 | 1.06 | 0.92 | 0.87 | 0.99 | 0.78 | 0.88 | 1.04 |
| | A | 0.79 | 0.84 | 0.62 | 0.89 | 0.97 | 0.99 | 0.96 | 1.05 | 0.95 | 0.91 | 1.02 | 0.98 |
| Large, Hydro-phobic | W | 0.87 | 0.71 | 0.69 | 0.68 | 0.97 | 0.83 | 0.83 | 0.68 | 0.62 | 0.68 | 0.28 | 1.01 |
| | V | 0.68 | 0.82 | 0.85 | 1.08 | 1.01 | 1.04 | 0.68 | 0.71 | 0.88 | 0.60 | 0.24 | 1.00 |
| | L | 1.06 | 1.01 | 0.41 | 0.89 | 0.68 | 0.90 | 0.90 | 0.69 | 0.89 | 0.82 | 0.21 | 0.79 |
| | I | 0.96 | 0.80 | 1.00 | 1.09 | 0.79 | 0.68 | 0.58 | 0.92 | 1.07 | 0.68 | 0.32 | 1.08 |

| IL-1β | Sub. Amino Acid | HH2 Sequence | | | | | | | | | | | |
|---|---|---|---|---|---|---|---|---|---|---|---|---|---|
| | | V | Q | L | R | I | R | V | A | V | I | R | A |
| Cationic | R | 0.93 | 0.70 | 0.82 | 0.90 | 1.10 | 0.90 | 1.04 | 0.43 | 0.97 | 0.88 | 0.90 | 0.69 |
| | K | 0.61 | 0.41 | 0.81 | 0.37 | 0.76 | 0.47 | 0.86 | 0.37 | 0.72 | 0.94 | 0.70 | 0.49 |
| Polar | Q | 0.68 | 0.90 | 0.73 | 0.45 | 0.80 | 0.63 | 0.86 | 0.72 | 0.71 | 0.76 | 0.73 | 0.63 |
| Small, Hydro-phobic | G | 1.00 | 0.95 | 1.23 | 1.14 | 1.27 | 0.90 | 1.08 | 1.15 | 1.20 | 1.11 | 1.05 | 1.03 |
| | A | 1.09 | 0.63 | 0.96 | 1.02 | 1.02 | 0.62 | 0.88 | 0.90 | 1.00 | 1.08 | 1.00 | 0.90 |
| Large, Hydro-phobic | W | 0.44 | 0.65 | 0.38 | 0.30 | 0.56 | 0.40 | 0.61 | 0.27 | 0.51 | 0.80 | 0.81 | 0.27 |
| | V | 0.90 | 0.55 | 0.71 | 0.43 | 0.82 | 0.33 | 0.90 | 0.32 | 0.90 | 0.71 | 0.81 | 0.48 |
| | L | 0.57 | 0.52 | 0.90 | 0.40 | 0.59 | 0.43 | 0.64 | 0.34 | 0.60 | 0.64 | 0.59 | 0.20 |
| | I | 0.49 | 0.49 | 0.59 | 0.39 | 0.90 | 0.46 | 0.38 | 0.40 | 0.46 | 0.90 | 0.61 | 0.36 |

C

| MCP-1 | Sub. Amino Acid | 1002 Sequence | | | | | | | | | | | |
|---|---|---|---|---|---|---|---|---|---|---|---|---|---|
| | | V | Q | R | W | L | I | V | W | R | I | R | K |
| Cationic | R | 0.9 | 2.1 | 0.8 | 0.3 | 0.8 | 0.3 | 1.3 | 0.4 | 0.8 | 0.5 | 0.8 | 0.5 |
| | K | 2.8 | 0.7 | 0.5 | 0.4 | 1.0 | 0.2 | 0.3 | 0.8 | 0.4 | 0.3 | 0.8 | 0.8 |
| Polar | Q | 0.8 | 0.8 | 0.4 | 3.4 | 7.4 | 3.9 | 2.4 | 0.4 | 2.2 | 0.4 | 3.9 | 0.7 |
| Small, Hydro-phobic | G | 2.3 | 0.6 | 1.7 | 6.9 | 0.4 | 0.2 | 0.2 | 0.5 | 1.6 | 0.6 | 0.5 | 0.2 |
| | A | 2.1 | 1.6 | 0.6 | 0.3 | 0.3 | 0.4 | 0.3 | 0.4 | 2.0 | 0.9 | 0.6 | 0.4 |
| Large, Hydro-phobic | W | 0.7 | 1.7 | 0.7 | 0.8 | 0.3 | 0.3 | 0.4 | 0.8 | 0.4 | 1.3 | 0.3 | 0.5 |
| | V | 0.8 | 2.2 | 0.4 | 1.7 | 4.7 | 0.7 | 0.8 | 1.3 | 0.4 | 0.4 | 0.5 | 0.3 |
| | L | 1.4 | 1.8 | 0.4 | 1.0 | 0.8 | 0.6 | 0.5 | 1.5 | 0.3 | 0.5 | 1.1 | 0.6 |
| | I | 5.6 | 0.9 | 1.6 | 0.6 | 2.9 | 0.8 | 0.5 | 1.1 | 0.5 | 0.8 | 0.5 | 0.3 |

| MCP-1 | Sub. Amino Acid | HH2 Sequence | | | | | | | | | | | |
|---|---|---|---|---|---|---|---|---|---|---|---|---|---|
| | | V | Q | L | R | I | R | V | A | V | I | R | A |
| Cationic | R | 1.6 | 0.5 | 3.7 | 0.5 | 0.6 | 0.5 | 0.3 | 0.9 | 0.5 | 5.2 | 0.5 | 3.1 |
| | K | 0.6 | 0.6 | 0.8 | 0.8 | 0.8 | 8.2 | 8.5 | 1.1 | 0.3 | 0.5 | 1.9 | 2.0 |
| Polar | Q | 3.9 | 0.5 | 0.5 | 0.3 | 0.4 | 11.0 | 0.4 | 0.7 | 2.1 | 2.0 | 1.2 | 1.2 |
| Small, Hydro-phobic | G | 0.3 | 0.6 | 0.3 | 8.6 | 10.3 | 0.7 | 0.2 | 10.3 | 0.4 | 4.3 | 0.3 | 4.1 |
| | A | 1.0 | 2.2 | 0.2 | 1.4 | 0.3 | 10.3 | 0.2 | 0.5 | 0.3 | 0.3 | 0.6 | 0.5 |
| Large, Hydro-phobic | W | 2.2 | 0.8 | 1.4 | 1.5 | 0.9 | 0.4 | 0.7 | 4.8 | 2.1 | 2.0 | 1.0 | 2.9 |
| | V | 0.5 | 1.6 | 12.3 | 3.0 | 0.7 | 4.5 | 0.5 | 3.0 | 0.5 | 2.2 | 0.6 | 2.1 |
| | L | 3.3 | 3.9 | 0.5 | 1.4 | 0.2 | 0.6 | 11.3 | 6.5 | 2.5 | 3.0 | 2.5 | 6.5 |
| | I | 3.1 | 10.8 | 9.0 | 0.8 | 0.5 | 0.6 | 0.8 | 1.2 | 3.6 | 0.5 | 3.5 | 1.4 |

**Fig. 1.** Biological activity summary of single amino acid substituted peptides. Amino acid substitution matrices for IDR-1002 (left) and IDR-HH2 (right) derivatives for antibiofilm activity against MRSA biofilms (A), suppression of pro-inflammatory cytokine IL-1β produced by PBMCs stimulated with *P. aeruginosa* PAO1 LPS (B) and of MCP-1 release from PBMCs (C). Antibiofilm activity is the percent of MRSA biofilm grown in the presence of peptide compared to the absence of peptide. IL-1β suppression is presented as the amount of cytokine produced in the presence of peptide compared to the amount of IL-1β produced by LPS stimulated PBMCs alone (defined as 1). MCP-1 is the average chemokine produced in ng/ml from all the biological replicates. Each set of peptides has been compared only to those peptides derived from the same parent sequence (either IDR-1002 or IDR-HH2, respectively). The peptides for each activity screen were colored from most active (top 25th percentile in red) to moderately active (white) and least active (bottom 75th percentile in gray). (For interpretation of the references to color in this figure legend, the reader is referred to the web version of this article.)

R9 appeared to be essential for the antibiofilm activity of IDR-1002 since all other residues (except W) caused a large decrease in antibiofilm activity. It was evident that residues near the N- and C-terminus had a lesser impact on the biological activity since substitutions at these positions were mostly highly active (highlighted in red). This indicated that the residues near the ends of the peptides could be readily swapped for other side chain moieties with relatively little impact on the antibiofilm activity of IDR-1002.

In the case of IDR-HH2, the substitution matrix for the antibiofilm activity revealed that the LRIRV stretch from position 3 to position 7 was particularly important for antibiofilm activity. Mutating any of the hydrophobic residues in this region to cationic or polar residues dramatically decreased the antibiofilm activity, while positively charged residues (either R or K) appeared to be essential at positions 4 and 6. In agreement with the IDR-1002 results, the residues at the ends of IDR-HH2 could largely be altered without negatively affecting the antibiofilm activity.

In a similar fashion, the immunomodulatory activity of all of the IDR-1002 and IDR-HH2 on human PBMCs was assessed at three different concentrations. These were again ranked according to their ability to suppress IL-1β production in the presence of LPS or stimulate MCP-1 production (Supplementary Figure 2). Compared to the IDR-HH2 derived peptides, it was clear that the IDR-1002 derivatives were better suppressors of LPS-induced IL-1β production. Thus, the substitution matrices for IL-1β suppression (Fig. 1B) were generated using data obtained at ~2 μM for the IDR-1002 derivatives and ~20 μM for IDR-HH2 derivatives.

In general, it appeared that for substituted peptides to reduce LPS induced IL-1β production, additional hydrophobic residues were preferred over cationic residues. Interestingly, there was a remarkable similarity between the residues that suppressed LPS-induced IL-1β production and those that contributed to antibiofilm activity. For example, mutating any of the residues between W4 and W9 in IDR-1002 to cationic or polar residues negatively impacted the suppression of IL-1β. This overlapped with the hydrophobic

**Table 1**
Peptide names and sequences. Residues changed in the derivative peptides relative to the parent peptide are indicated in bold and by underlining. The antibiofilm activity of the peptides against MRSA are shown as $MBIC_{50}$, which corresponds to the minimum peptide concentration required to inhibit 50% of MRSA biofilm growth.

| Peptide | Sequence | $MBIC_{50}$ (μg/ml) |
|---|---|---|
| IDR-1002 | VQRWLIVWRIRK | 10 |
| IDR-2009 | **K**W**R**L**R**WRI**Q**K | 5 |
| IDR-2010 | **K**QRWLI**R**WRIRK | 20 |
| IDR-HH2 | VQLRIRVAVIRA | 40 |
| IDR-2011 | VQLRIRV**K**VIR**K** | 80 |
| IDR-2012 | **W**QLRIRV**K**VIR**K** | 40 |
| IDR-2013 | **W**Q**RVR**RV**K**VIR**K** | >80 |

stretch found to be important for the antibiofilm activity of IDR-1002. For the IDR-HH2 derived peptides, it was apparent that the residues encompassing LRIRV were again important to the ability to suppress IL-1β production and that increasing the hydrophobic character in this region yielded peptides with enhanced activity. Interestingly, in IDR-HH2 derivatives, neither of the small hydrophobic amino acids (Gly and Ala) improved the ability to suppress IL-1β.

Lastly, the MCP-1 produced by PBMCs at the highest peptide concentration was used to generate substitution matrices for IDR-1002 and IDR-HH2 (Fig. 1C) since this concentration resulted in the greatest spread of activities. It is important to note that there was a significant amount of PBMC-donor variability in the amount of chemokine generated in response to each peptide derivative, resulting in very large standard errors (Supplementary Figure 2, bottom panel). This variation might have contributed to the relatively disordered substitution matrices obtained for the MCP-1 activities of IDR-1002 and IDR-HH2 (Fig. 1C). While it was clear that certain residues were favored over others, it was difficult to identify key residues that significantly contributed to chemokine induction. The differences seen in the MCP-1 substitution matrices compared to the matrices for antibiofilm and IL-1β suppression suggested that the sequence characteristics of a peptide capable of inducing chemokine production were distinct from those contributing to the pro-inflammatory suppression properties and the antibiofilm potency.

### *Antibiofilm activity of second generation peptides*

The substitution matrices obtained from the high-throughput screens were used to inform the synthesis of next generation peptides with enhanced biological activity compared to the parent peptides. In this case, we chose to focus on combining mutations to IDR-1002 and IDR-HH2 that would enhance MCP-1 production while also improving (if possible) or not dramatically reducing the antibiofilm activity or proinflammatory cytokine suppression activities of the peptides. MCP-1 optimization was chosen as the driving force behind the selection of mutations for the second-generation peptides because both of the parent peptides exhibited weak MCP-1 induction ability. In total, two IDR-1002 derivatives and three IDR-HH2 derivatives were chemically synthesized and obtained at high purity (Table 1).

Both second generation IDR-1002 derived peptides had similar antibiofilm activity compared with their parent peptide using the static microtitre assay used to screen the SPOT-synthesized peptides. IDR-2009 exhibited a two-fold improvement in $MBIC_{50}$ compared to IDR-1002 while IDR-2010 was only two-fold less active compared to IDR-1002 (Table 1). IDR-HH2 alone proved to be a much weaker antibiofilm peptide compared to IDR-1002 with an observed $MBIC_{50}$ of 40 μg/ml. Two of the IDR-HH2 derived peptides, IDR-2011 and IDR-2012, exhibited similar antibiofilm activity to their parent sequence; however, IDR-2013, which had the greatest number of altered residues compared to the parent sequence, proved to be inactive against MRSA biofilms at peptide concentrations below 80 μg/ml (Table 1).

The antibiofilm activity of IDR-2009 and IDR-2013 as well as the parent peptides, was further examined against biofilms grown under flow cell conditions, which is a more accurate and sensitive assay of biofilm inhibition. Both IDR-1002 and IDR-2009 demonstrated a potent ability to eradicate preformed MRSA biofilms compared to untreated controls. At peptide concentrations of 1.25 μg/ml, only a few cells persisted in the flow cells while almost all of the biofilm was destroyed above 2.5 μg/ml (Fig. 2). IDR-HH2 was less active than the IDR-1002 derived peptides, but peptide treatment in flow cells still resulted in biofilm eradication at 5 μg/ml while most of the remaining cells at 2.5 μg/ml were co-stained with the SYTO-9 and propidium iodide dyes, suggesting that the cells were mostly dead (Fig. 2). In agreement with the static microtitre biofilm assay results, IDR-2013 did not have a significant effect on MRSA biofilms grown under flow cell conditions (Fig. 2).

Since biofilms associated with skin infections are likely to consist of multiple bacterial species, these four peptides were also tested for their ability to eradicate preformed biofilms formed by *P. aeruginosa* PAO1. *P. aeruginosa* is a Gram negative opportunistic pathogen that readily forms biofilms [42] and this species of bacteria has been isolated from chronic dermal wounds [43,44]. Interestingly, IDR-1002 and IDR-2009 demonstrated potent antibiofilm activity and virtually abolished all of the PAO1 biofilm at 2.5 μg/ml (Fig. 3). Conversely, IDR-HH2 and IDR-2013 had little effect on PAO1 biofilms at 2.5 μg/ml. This was expected for IDR-2013, as this peptide lacked antibiofilm activity against MRSA biofilms; however, the lack of activity for IDR-HH2 suggests that differences in biofilm structure and organization between bacterial species also influences the antibiofilm effectiveness of peptides.

### *Immunomodulatory and cytotoxic activity of second generation peptides*

The immunomodulatory activity and cytotoxicity of the second generation peptides was evaluated on human PBMCs. Both of the IDR-1002 derived peptides caused MCP-1 release from PBMCs in a dose dependent manner (Fig. 4A, top panel). More importantly, compared to parent peptide IDR-1002, both IDR-2009 and IDR-2010 induced more MCP-1, demonstrating that efforts made to enhance the MCP-1 production were successful. Conversely, the IDR-HH2 derived peptides did not exhibit an increased ability to stimulate MCP-1 production. Instead, IDR-2012 proved only slightly more stimulatory than IDR-HH2 at 50 μg/ml, while the biological activity of IDR-2011 was almost equivalent to the parent peptide (Fig. 4B, top panel). Interestingly, the ability to induce MCP-1 production was virtually abolished in IDR-2013.

In general, all of the parent and second-generation peptides suppressed LPS-induced IL-1β production in a dose dependent manner with the exception of IDR-2013, which did not suppress IL-1β production at any concentration tested (Fig. 4, middle panel). When compared to their parent peptides, IDR-2009 appeared to be slightly better than IDR-1002 at all three concentrations tested while peptide IDR-2010 was slightly worse (Fig. 4). In general, the IDR-HH2 derived peptides possessed weaker anti-inflammatory properties compared to the IDR-1002 derived peptides, which is in agreement with the results seen in the immunomodulatory screen. Once again, IDR-2013 lacked any appreciable activity as it did not suppress IL-1β production from LPS stimulated PBMCs.

Up to this point, the cytotoxic activity of the IDR-1002 and IDR-HH2 derived peptides had not been considered. However, for peptides to have therapeutic potential, they need to lack cytotoxic activity toward normal human cells. The LDH-release assay was

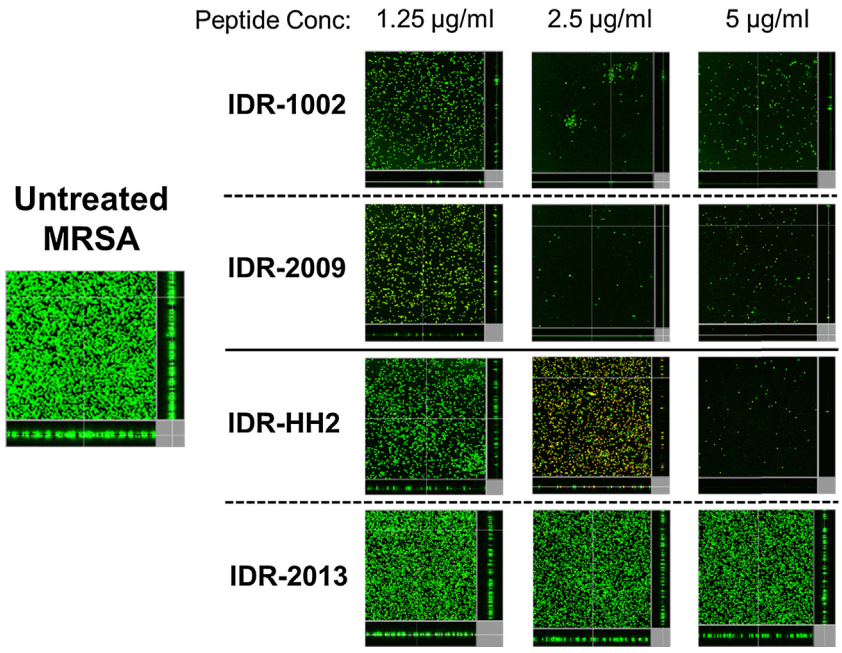


**Fig. 2.** Antibiofilm activity of peptides against MRSA biofilms. Confocal microscopy images of MRSA biofilms grown in flow cells and treated with IDR-1002 or IDR-HH2 as well as their respective derivatives IDR-2009 and IDR-2013. Peptides were tested for their ability to eradicate pre-formed biofilms at concentrations of 1.25, 2.5 and 5 μg/ml. The biofilms were stained with SYTO-9 dye that stains all cells green, as well as propidium iodide which selectively stains dead cells red. (For interpretation of the references to color in this figure legend, the reader is referred to the web version of this article.)

used to assess the cytotoxicity of all the second-generation peptides against PBMCs as well as the parent peptides. Overall, most of the peptides were not toxic (Fig. 4, bottom panel). Two of the peptides, namely IDR-2009 and IDR-2012, exhibited a small dose dependent increase in cytotoxicity with up to 30% and 40% LDH release occurring respectively at 50 μg/ml (Fig. 4, bottom panel).

*Structural characterization of second generation peptides*

IDR-2009 and IDR-2013 as well as the parent peptides IDR-1002 and IDR-HH2, were structurally characterized using circular dichroism spectroscopy. Except for the inactive peptide IDR-2013, the peptides were unstructured in phosphate buffer and then adopted different conformations in the presence of the SDS or DPC detergents (Fig. 5). IDR-1002 and IDR-2009 both adopted more helical conformations in the presence of micelles based on the characteristic minima observed at 208 and 222 nm as well as the maxima at 190 nm. The type of micelle did not affect the overall conformation of these two peptides since the spectra were virtually identical under both conditions. IDR-HH2 also changed conformation in the presence of micelles; however, the structure adopted by the peptide depended on the type of micelle, being α-helical with anionic SDS micelles and β-structured with neutral DPC micelles. IDR-2013 remained unstructured under all three conditions

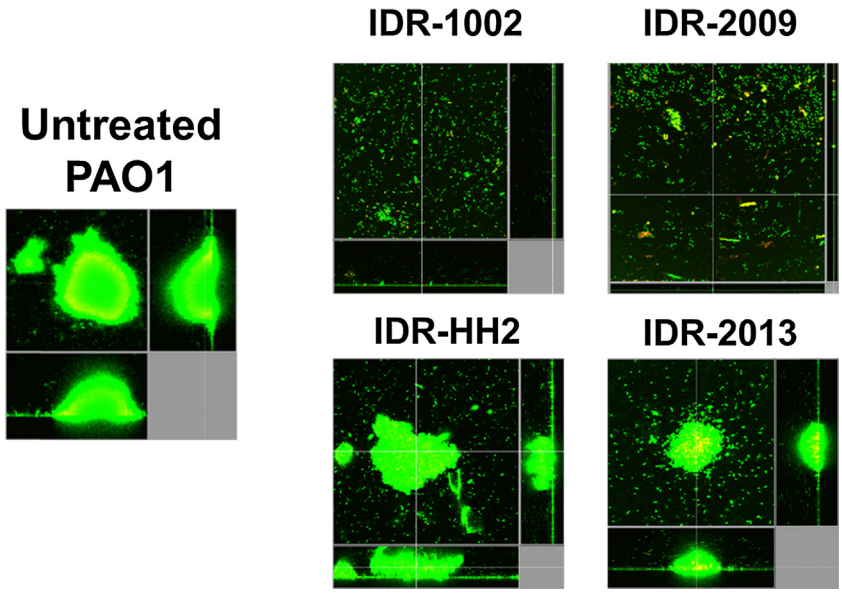


**Fig. 3.** Antibiofilm activity, against *P. aeruginosa* PAO1, of selected second generation peptides and their parent peptides. All peptides were added to two-day old biofilms and were tested at a concentration of 2.5 μg/ml.

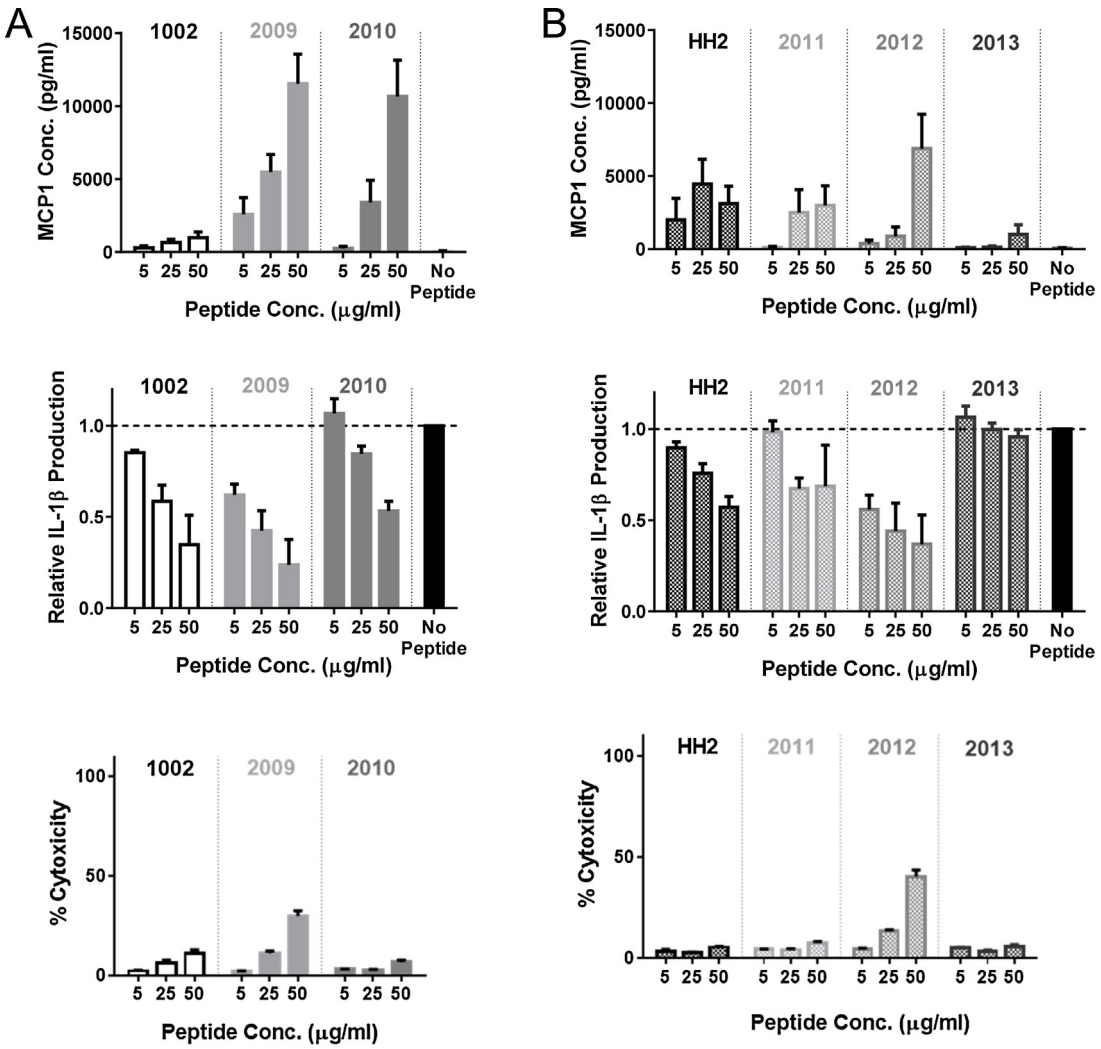


**Fig. 4.** Immunomodulatory and cytotoxic activities of IDR-1002 (A) and IDR-HH2 (B) derivatives. Peptide induced MCP-1 production in PBMCs was evaluated (top panels, 8 biological replicates) as well as the suppression of LPS-induced IL-1β (middle panels, 4 biological replicates) compared to LPS-stimulated PBMCs treated with the vehicle control (defined as having a value of 1.0). The cytotoxicity of the peptides was also evaluated against PBMCs using the LDH-release assay (bottom panels, 5 biological replicates). Each peptide was tested at 5, 25 and 50 μg/ml. The data shown represent the mean of the biological replicates ± SEM.

indicating that IDR-2013 was unable to fold into and associate with micelles.

## Discussion

MRSA is a major cause of hospital and community-acquired infections, resulting in many device-related and wound infections; all of which can be attributed to formation of highly resistant biofilms. Given the lack of effective therapies, MRSA biofilm infections are associated with a high rate of morbidity, and as such, are an immense problem for public health. An ideal peptide therapeutic to treat MRSA associated skin infections would possess potent antibiofilm activity to either disperse or directly attack the MRSA cells within the biofilm while also suppressing the harmful effects of inflammation that are associated with bacterial infections. In addition, the ability to induce chemokines that attract monocytes to the site of infection would tend to further enhance the body's own defenses to fight off the infection.

In the present work, we set out to optimize two peptides, IDR-1002 and IDR-HH2, for their antibiofilm and immunomodulatory activities. To accomplish this, single amino acid substitution analysis was performed on both sequences using SPOT-synthesized peptide arrays on cellulose membranes, substituting one of nine different amino acids at every position along the length of both peptide sequences. A similar strategy was previously used to successfully optimize AMP sequences for antibacterial activity against *E. coli* and *S. aureus* [45]. Here, second-generation peptides that combined the most favorable substitutions were generated taking into account three distinct biological activities that are known to be independent of antimicrobial activity vs. planktonic cells, namely antibiofilm activity against MRSA biofilms, ability to suppress LPS-induced IL-1β production from human PBMCs and induction of MCP-1 from PBMCs. Ultimately, a novel peptide, IDR-2009, was generated that possessed an overall improved biological activity profile compared to its parent peptide.

In contrast to IDR-2009, the second generation peptide IDR-2013 lost most of its biological activity. Half of the residues in IDR-HH2 were mutated to create IDR-2013, making it the most altered second generation peptide examined in this study. The structural characterization with CD spectroscopy indicated that IDR-2013 did not interact with membrane-mimicking detergent micelles. This suggests that it is incapable of interacting with biological membranes, which is likely a necessary component of its antibiofilm and immunomodulatory mechanisms of action. The results for IDR-2013, cf. other peptides, are consistent with the concept that the biological activity of a peptide is determined by

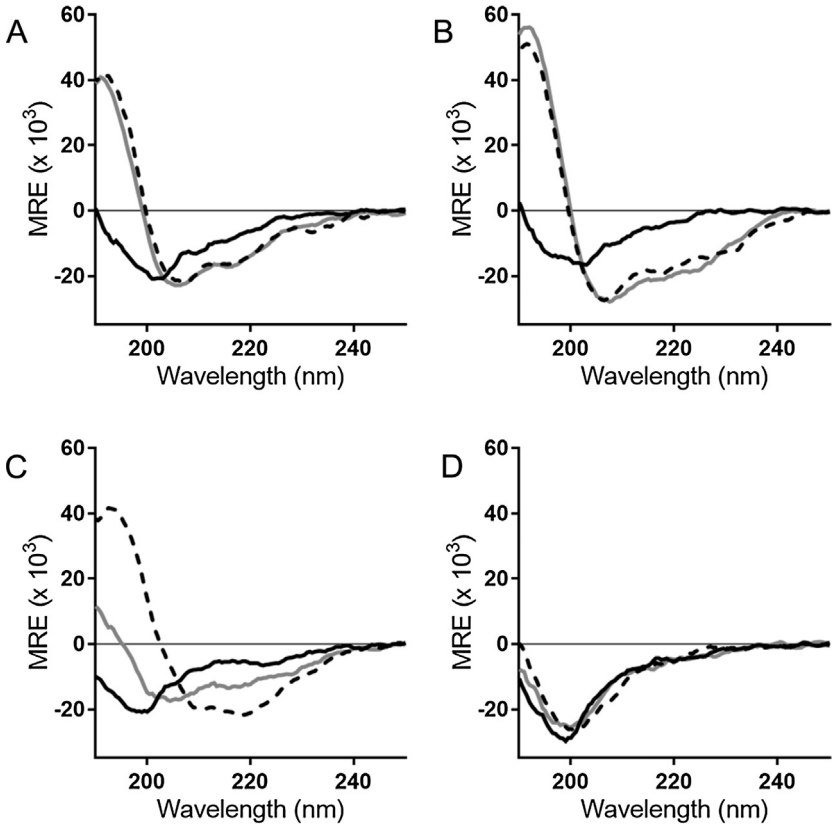


**Fig. 5.** Circular dichroism spectra of IDR-1002 (A), IDR-2009 (B), IDR-HH2 (C) and IDR-2013 (D). Spectra were acquired on 25 μM peptide samples in sodium phosphate buffer (black line) and in the presence of 10 mM DPC (gray line) or 25 mM SDS micelles (dashed line). CD spectra are expressed in terms of mean residue ellipticity (MRE) with units of deg cm$^2$ dmol$^{-1}$ res$^{-1}$.

its specific amino acid sequence and ability to interact with membranes. Small mutations in any given sequence are likely to fine tune the physicochemical properties of the peptide and have an incremental effect on the biological activity. Thus, while IDR-2013 had a number of changes that were independently favorable, the overall effect of these changes was to substantially decrease the overall hydrophobicity, which prevented interaction with membranes and/or restructuring.

There are some inherent experimental limitations associated with this methodology. The first is that the starting peptide sequences should have at least some measurable activity at the peptide concentration that can be evaluated. If a high peptide concentration is required to elicit a biological response, then SPOT-synthesized peptides might not yield sufficient quantities for assessing all of the desired biological replicates. This could be addressed in part by combining peptide yields from multiple identical peptide spots on SPOT-synthesized arrays. Secondly, the use of human PBMCs introduces significant biological variability to the immunomodulatory activity data (See Supplementary Figure 2) which could lead to variations between repeat studies. This is an inherent problem with using human samples due to the large variation that exists among the general population. Although immortal cell lines could potentially be used in place of PBMCs, especially in cases where the biological variation is extremely large (such as the MCP-1 production measured in the present study) we have not identified a cell line that is as responsive as primary cells. Moreover, it is unclear if the peptide response induced in cell lines follows the same patterns as the immunomodulatory response from human PBMCs or whether a single cell can mimic the effects of a mixture of cells, which is of course what occurs in the body. Thirdly, the SPOT-synthesis technique yields peptides at a lower purity compared to those obtained from conventional solid phase synthesis techniques. Therefore, it is possible that some of these impurities (each present at relatively modest concentrations) might contribute significantly to the observed biological activities of the screened peptides. It is for this reason that any peptide derived from the information found in the substitution matrices needs to be synthesized at high purity and its improved biological activity validated separately. Finally, this method does not account for unexpected increases in secondary peptide characteristics, such as the increase in cytotoxicity observed for IDR-2009 and IDR-2012. In principle, it may be possible to include more peptide activities such as toxicity in the initial screens, provided sufficient peptide is available. These additional activities could then be incorporated into the design of next generation peptides.

The advantages of using this approach to optimize bioactive peptides are numerous. The most obvious is the decreased cost of peptide synthesis compared to conventional larger scale synthesis methods. Commercially obtaining 2 mg of synthetic peptide at 80% purity from the same company that prepared the peptide arrays would cost $120 per sequence. This means that it would cost approximately $24,000 to obtain all of the sequences used in the substitution analysis studies described here. In comparison, the SPOT-synthesized arrays used in this study cost ~$2,000. It is worth mentioning that most of these mutated sequences would likely be less active than the starting peptide, meaning that the majority of the synthetic peptide would go to waste as they would have no therapeutic relevance. In addition, both the original peptides as well as optimized peptides that combined the most favorable mutations would still need to be synthesized at high purity to confirm their activity and to investigate them in more detail. Data obtained from these studies can also be used to establish quantitative structure

activity relationships (QSAR) for each activity that can be used to computationally model and predict the activity of virtual peptide libraries in silico [46]. These virtual peptide libraries can be structurally modeled using physico-chemical "descriptors" and, based on neural network models created using defined test sets, enable the in silico screening of hundreds of thousands of peptides and ranking them according to their predicted biological activities. The most active sequences can then be SPOT-synthesized on cellulose sheets and their activity can be measured as described here to confirm the results from the computational predictions and identify completely novel peptides that are fine tuned for their antibiofilm and immunomodulatory activities. This process can also be repeated iteratively to further enhance our understanding of the molecular descriptors that define the antibiofilm and immunomodulatory activities of synthetic IDR peptides. Finally, the process of peptide optimization described here could potentially be used to enhance a peptide sequence for any type of activity, provided there is a functional assay that can be easily developed for high throughput testing. Examples of other peptides that might benefit from such a strategy include anticancer peptides [47], antiviral peptides [48] and drug delivering cell penetrating peptides [49].

The method described here dramatically streamlines the process of identifying peptides with good antibiofilm and immunomodulatory activity. It provides a cost effective method to simultaneously assess the biological activity of hundreds of peptides and successfully generated a novel synthetic peptide, IDR-2009, with an enhanced biological activity profile. Preliminary studies suggest that IDR-2009 is well tolerated in mice (data not shown) and further animal studies will need to be conducted to validate the safety and efficacy of these synthetic peptides as novel drug therapies.

## Acknowledgements

This work was supported by the Canadian Institutes of Health Research (CIHR) [funding reference number MOP-74493]. Research reported in this publication was also supported by the National Institute of Allergy and Infectious Diseases of the National Institutes of Health under Award Number R33AI098701. The content is solely the responsibility of the authors and does not necessarily represent the official views of the National Institutes of Health. The Jasco CD Spectropolarimeter was provided through grants from the Canadian Foundation for Innovation and the Michael Smith Foundation to the Laboratory of Molecular Biophysics. EFH and ALH are both recipients of postdoctoral fellowships from CIHR. CdlF-N received a scholarship from the Fundación "la Caixa" and Fundación Canada (Spain). REWH holds a Canada Research Chair.

## Appendix A. Supplementary data

Supplementary material related to this article can be found, in the online version, at http://dx.doi.org/10.1016/j.peptides.2015.03.015.

## References

[1] Zanger P, Holzer J, Schleucher R, Steffen H, Schittek B, Gabrysch S. Constitutive expression of the antimicrobial peptide RNase 7 is associated with *Staphylococcus aureus* infection of the skin. J Infect Dis 2009;200:1907–15, http://dx.doi.org/10.1086/648408.

[2] Otto M. Staphylococcus colonization of the skin and antimicrobial peptides. Expert Rev Dermatol 2010;5:183–95, http://dx.doi.org/10.1586/edm.10.6.

[3] Dantes R, Mu Y, Belflower R, Aragon D, Dumyati G, Harrison LH, et al. National burden of invasive methicillin-resistant *Staphylococcus aureus* infections, United States, 2011. JAMA Intern Med 2013;173:1970–8, http://dx.doi.org/10.1001/jamainternmed.2013.10423.

[4] Filice GA, Nyman JA, Lexau C, Lees CH, Bockstedt LA, Como-Sabetti K, et al. Excess costs and utilization associated with methicillin resistance for patients with *Staphylococcus aureus* infection. Infect Control Hosp Epidemiol 2010;31:365–73, http://dx.doi.org/10.1086/651094.

[5] Weigel LM, Clewell DB, Gill SR, Clark NC, McDougal LK, Flannagan SE, et al. Genetic analysis of a high-level vancomycin-resistant isolate of *Staphylococcus aureus*. Science 2003;302:1569–71, http://dx.doi.org/10.1126/science.1090956.

[6] Rossi F, Diaz L, Wollam A, Panesso D, Zhou Y, Rincon S, et al. Transferable vancomycin resistance in a community-associated MRSA lineage. N Engl J Med 2014;370:1524–31, http://dx.doi.org/10.1056/NEJMoa1303359.

[7] Mansour SC, Pena OM, Hancock REW. Host defense peptides: front-line immunomodulators. Trends Immunol 2014;35:443–50, http://dx.doi.org/10.1016/j.it.2014.07.004.

[8] Nguyen LT, Haney EF, Vogel HJ. The expanding scope of antimicrobial peptide structures and their modes of action. Trends Biotechnol 2011;29:464–72, http://dx.doi.org/10.1016/j.tibtech.2011.05.001.

[9] Hancock REW, Diamond G. The role of cationic antimicrobial peptides in innate host defences. Trends Microbiol 2000;8:402–10.

[10] Hancock REW, Sahl HG. Antimicrobial and host-defense peptides as new anti-infective therapeutic strategies. Nat Biotechnol 2006;24:1551–7.

[11] Ommori R, Ouji N, Mizuno F, Kita E, Ikada Y, Asada H. Selective induction of antimicrobial peptides from keratinocytes by staphylococcal bacteria. Microb Pathog 2013;56:35–9, http://dx.doi.org/10.1016/j.micpath.2012.11.005.

[12] Sass V, Schneider T, Wilmes M, Körner C, Tossi A, Novikova N, et al. Human beta-defensin 3 inhibits cell wall biosynthesis in Staphylococci. Infect Immun 2010;78:2793–800, http://dx.doi.org/10.1128/IAI.00688-09.

[13] Ong PY, Ohtake T, Brandt C, Strickland I, Boguniewicz M, Ganz T, et al. Endogenous antimicrobial peptides and skin infections in atopic dermatitis. N Engl J Med 2002;347:1151–60, http://dx.doi.org/10.1056/NEJMoa021481.

[14] Zanger P, Nurjadi D, Vath B, Kremsner PG. Persistent nasal carriage of *Staphylococcus aureus* is associated with deficient induction of human β-defensin 3 after sterile wounding of healthy skin in vivo. Infect Immun 2011;79:2658–62, http://dx.doi.org/10.1128/IAI.00101-11.

[15] Haney EF, Hancock RBEW. Peptide design for antimicrobial and immunomodulatory applications. Biopolymers 2013;100:572–83, http://dx.doi.org/10.1002/bip.22250.

[16] Haisma EM, de Breij A, Chan H, van Dissel JT, Drijfhout JW, Hiemstra PS, et al. LL-37-derived peptides eradicate multidrug-resistant *Staphylococcus aureus* from thermally wounded human skin equivalents. Antimicrob Agents Chemother 2014;58:4411–9, http://dx.doi.org/10.1128/AAC.02554-14.

[17] Björn C, Håkansson J, Myhrman E, Sjöstrand V, Haug T, Lindgren K, et al. Anti-infectious and anti-inflammatory effects of peptide fragments sequentially derived from the antimicrobial peptide centrocin 1 isolated from the green sea urchin, *Strongylocentrotus droebachiensis*. AMB Express 2012;2:67, http://dx.doi.org/10.1186/2191-0855-2-67.

[18] Lopez D, Vlamakis H, Kolter R. Biofilms. Cold Spring Harb Perspect Biol 2010;2:a000398.

[19] Davis SC, Ricotti C, Cazzaniga A, Welsh E, Eaglstein WH, Mertz PM. Microscopic and physiologic evidence for biofilm-associated wound colonization in vivo. Wound Repair Regen 2008;16:23–9, http://dx.doi.org/10.1111/j.1524-475X.2007.00303.x.

[20] Percival SL, Hill KE, Williams DW, Hooper SJ, Thomas DW, Costerton JW. A review of the scientific evidence for biofilms in wounds. Wound Repair Regen 2012;20:647–57, http://dx.doi.org/10.1111/j.1524-475X.2012.00836.x.

[21] De la Fuente-Núñez C, Reffuveille F, Fernández L, Hancock RE. Bacterial biofilm development as a multicellular adaptation: antibiotic resistance and new therapeutic strategies. Curr Opin Microbiol 2013;16:580–9, http://dx.doi.org/10.1016/j.mib.2013.06.013.

[22] Costerton JW, Stewart PS, Greenberg EP. Bacterial biofilms: a common cause of persistent infections. Science 1999;284:1318–22.

[23] Overhage J, Campisano A, Bains M, Torfs EC, Rehm BH, Hancock REW. Human host defense peptide LL-37 prevents bacterial biofilm formation. Infect Immun 2008;76:4176–82.

[24] De la Fuente-Nunez C, Korolik V, Bains M, Nguyen U, Breidenstein EB, Horsman S, et al. Inhibition of bacterial biofilm formation and swarming motility by a small synthetic cationic peptide. Antimicrob Agents Chemother 2012;56:2696–704.

[25] De la Fuente-Núñez C, Reffuveille F, Haney EF, Straus SK, Hancock REW. Broad-spectrum anti-biofilm peptide that targets a cellular stress response. PLoS Pathog 2014;10:e1004152, http://dx.doi.org/10.1371/journal.ppat.1004152.

[26] Bowdish DM, Davidson DJ, Lau YE, Lee K, Scott MG, Hancock REW. Impact of LL-37 on anti-infective immunity. J Leukoc Biol 2005;77:451–9.

[27] Hilchie AL, Wuerth K, Hancock REW. Immune modulation by multifaceted cationic host defense (antimicrobial) peptides. Nat Chem Biol 2013;9:761–8, http://dx.doi.org/10.1038/nchembio.1393.

[28] Wieczorek M, Jenssen H, Kindrachuk J, Scott WR, Elliott M, Hilpert K, et al. Structural studies of a peptide with immune modulating and direct antimicrobial activity. Chem Biol 2010;17:970–80.

[29] Steinstraesser L, Hirsch T, Schulte M, Kueckelhaus M, Jacobsen F, Mersch EA, et al. Innate defense regulator peptide 1018 in wound healing and wound infection. PLOS ONE 2012;7:e39373.

[30] Nijnik A, Madera L, Ma S, Waldbrook M, Elliott MR, Easton DM, et al. Synthetic cationic peptide IDR-1002 provides protection against bacterial infections through chemokine induction and enhanced leukocyte recruitment. J Immunol 2010;184:2539–50.
[31] Turner-Brannen E, Choi KY, Lippert DN, Cortens JP, Hancock REW, El-Gabalawy H, et al. Modulation of interleukin-1beta-induced inflammatory responses by a synthetic cationic innate defence regulator peptide, IDR-1002, in synovial fibroblasts. Arthritis Res Ther 2011;13:R129.
[32] Madera L, Hancock REW. Synthetic immunomodulatory peptide IDR-1002 enhances monocyte migration and adhesion on fibronectin. J Innate Immun 2012;4:553–68.
[33] Rivas-Santiago B, Castañeda-Delgado JE, Rivas Santiago CE, Waldbrook M, González-Curiel I, León-Contreras JC, et al. Ability of innate defence regulator peptides IDR-1002, IDR-HH2 and IDR-1018 to protect against *Mycobacterium tuberculosis* infections in animal models. PLOS ONE 2013;8:e59119, http://dx.doi.org/10.1371/journal.pone.0059119.
[34] Brown THT, David J, Acosta-Ramirez E, Moore JM, Lee S, Zhong G, et al. Comparison of immune responses and protective efficacy of intranasal prime-boost immunization regimens using adenovirus-based and CpG/HH2 adjuvanted-subunit vaccines against genital *Chlamydia muridarum* infection. Vaccine 2012;30:350–60, http://dx.doi.org/10.1016/j.vaccine.2011.10.086.
[35] Kindrachuk J, Jenssen H, Elliott M, Townsend R, Nijnik A, Lee SF, et al. A novel vaccine adjuvant comprised of a synthetic innate defence regulator peptide and CpG oligonucleotide links innate and adaptive immunity. Vaccine 2009;27:4662–71.
[36] Frank R. The SPOT-synthesis technique. Synthetic peptide arrays on membrane supports – principles and applications. J Immunol Methods 2002;267:13–26.
[37] Hilpert K, Winkler DF, Hancock REW. Peptide arrays on cellulose support: SPOT synthesis, a time and cost efficient method for synthesis of large numbers of peptides in a parallel and addressable fashion. Nat Protoc 2007;2:1333–49.
[38] Winkler DF, Hilpert K, Brandt O, Hancock REW. Synthesis of peptide arrays using SPOT-technology and the CelluSpots-method. Methods Mol Biol 2009;570:157–74.
[39] Pitts B, Hamilton MA, Zelver N, Stewart PS. A microtiter-plate screening method for biofilm disinfection and removal. J Microbiol Methods 2003;54:269–76.
[40] Jahnsen RD, Haney EF, Franzyk H, Hancock REW. Characterization of a proteolytically stable multifunctional host defense peptidomimetic. Chem Biol 2013;20:1286–95, http://dx.doi.org/10.1016/j.chembiol.2013.09.007.
[41] Wallace BA, Janes RW. An introduction to circular dichroism and synchrotron radiation circular dichroism spectroscopy. In: Haris PI, editor. Mod. Tech. Circ. Dichroism Synchrotron Radiat. Circ. Dichroism Spectrosc. Amsterdam: IOS Press; 2009. p. 1–18.
[42] Gellatly SL, Hancock REW. *Pseudomonas aeruginosa*: new insights into pathogenesis and host defenses. Pathog Dis 2013;67:159–73, http://dx.doi.org/10.1111/2049-632X.12033.
[43] Gjødsbøl K, Christensen JJ, Karlsmark T, Jørgensen B, Klein BM, Krogfelt KA. Multiple bacterial species reside in chronic wounds: a longitudinal study. Int Wound J 2006;3:225–31, http://dx.doi.org/10.1111/j.1742-481X.2006.00159.x.
[44] Kirketerp-Møller K, Jensen PØ, Fazli M, Madsen KG, Pedersen J, Moser C, et al. Distribution, organization, and ecology of bacteria in chronic wounds. J Clin Microbiol 2008;46:2717–22, http://dx.doi.org/10.1128/JCM.00501-08.
[45] Hilpert K, Volkmer-Engert R, Walter T, Hancock REW. High-throughput generation of small antibacterial peptides with improved activity. Nat Biotechnol 2005;23:1008–12.
[46] Cherkasov A, Hilpert K, Jenssen H, Fjell CD, Waldbrook M, Mullaly SC, et al. Use of artificial intelligence in the design of small peptide antibiotics effective against a broad spectrum of highly antibiotic-resistant superbugs. ACS Chem Biol 2009;4:65–74.
[47] Hoskin DW, Ramamoorthy A. Studies on anticancer activities of antimicrobial peptides. Biochim Biophys Acta 2008;1778:357–75, http://dx.doi.org/10.1016/j.bbamem.2007.11.008.
[48] Barlow PG, Findlay EG, Currie SM, Davidson DJ. Antiviral potential of cathelicidins. Future Microbiol 2014;9:55–73, http://dx.doi.org/10.2217/fmb.13.135.
[49] Shi N-Q, Qi X-R, Xiang B, Zhang Y. A survey on "Trojan Horse" peptides: opportunities, issues and controlled entry to "Troy". J Control Release 2014;194C:53–70, http://dx.doi.org/10.1016/j.jconrel.2014.08.014.